Available online at www.sciencedirect.com
ScienceDirect
Chemistry and Physics of Lipids 144 (2006) 45–59
CPL
CHEMISTRY AND PHYSICS OF LIPIDS
www.elsevier.com/locate/chemphyslip

Crystallinity of plant epicuticular waxes: electron and X-ray diffraction studies

H.J. Ensikat [a], M. Boese [b], W. Mader [b], W. Barthlott [a], K. Koch [a,*]

[a] *Nees-Institut für Biodiversität der Pflanzen der Universität Bonn, Meckenheimer Allee 170, 53115 Bonn, Germany*
[b] *Institut für Anorganische Chemie der Universität Bonn, Römerstr. 164, 53117 Bonn, Germany*

Received 17 November 2005; accepted 19 June 2006
Available online 10 July 2006

Abstract

The crystal structure of the epicuticular waxes of 35 plant species has been examined by electron diffraction and X-ray powder diffraction. The waxes include the most common morphological wax types such as platelets, tubules, films and rodlets. Most of them were prepared with a special mechanical isolation method, which preserves the original crystal structure. Solvent-extracted recrystallized plant waxes were compared with mechanically isolated samples. The waxes were found to occur in three different crystal structures. Most of the waxes exhibited an orthorhombic structure which is the most common for aliphatic compounds. Tubules containing mainly secondary alcohols showed diffraction reflections of a triclinic phase; broad reflection peaks indicated a significant disorder. Ketones, in particular beta-diketone tubules, displayed the reflections of a hexagonal structure. Mixtures of different phases could be identified. For most of the waxes, the 'long spacing' diffraction reflections indicated a layer structure with the characteristics of the major component. Others showed no 'long spacing' reflections indicating a strong disorder of the molecular layers.

Keywords: Epicuticular wax; Plant waxes; Crystal structure; Electron diffraction; X-ray diffraction

1. Introduction

Most primary surfaces of higher plants, e.g. those of leaves and fruits, consist of a hydrophobic layer, composed of the cuticle and epicuticular waxes. The epicuticular waxes determine the surface characteristics, for example the anti-adhesive property of Lotus (*Nelumbo nucifera*) leaves (Barthlott and Neinhuis, 1997). They appear in many different morphological forms. On some species it is only a smooth wax film, others are covered with wax particles, which are often termed "crystalloids", in combination with a basal wax film. A morphological classification of the epicuticular waxes, based on extensive scanning electron microscopy (SEM) studies, has been published by Barthlott et al. (1998). For some wax types, e.g. platelets and tubules, a correlation between the chemical composition and the morphology was found (Baker, 1982; Meusel, 1997; Koch et al., 2006).

Broad overviews about early works on the chemistry of plant waxes are published by several authors, e.g. Kolattukudy (1976), Martin and Juniper (1970). Typical plant waxes are mixtures of long-chain aliphatic compounds: *n*-alkanes and their derivatives with an oxygen-containing functional group, mainly alcohols, ketones, aldehydes, fatty acids, or esters. The present study

* Corresponding author. Tel.: 49 228 739619; Fax: +49 228 733120.
E-mail address: koch@uni-bonn.de (K. Koch).

0009-3084/$ – see front matter © 2006 Elsevier Ireland Ltd. All rights reserved.
doi:10.1016/j.chemphyslip.2006.06.016

focuses on these characteristic aliphatic waxes, which are solid at room temperature and soluble in organic solvents. Besides these, other epicuticular coatings exist, e.g. insoluble polymerized crusts, liquid oily waxes containing unsaturated compounds and waxes with a high amount of triterpenoids or flavonoids.

The physical properties of the waxes, e.g. their solubility in organic solvents and defined melting point between 60 and 95 °C, suggest a crystalline order, which has, however, not yet been generally proved for all types of natural epicuticular waxes. Smooth wax layers are often named "amorphous wax films" (e.g. Jeffree, 1996), but this term is obviously used as a morphological but not a crystallographic characterization. The crystalline order can be analyzed in detail by X-ray diffraction (XRD) and electron diffraction (ED). XRD has frequently been used in the early studies of waxes as a tool for the identification of compounds isolated from natural waxes. The XRD powder diffraction diagrams contain information about lattice parameters, the chain length of the molecules and the position of oxygen-containing functional groups (overviews in Malkin, 1952; Mazliak, 1968). Most previous XRD studies of plant waxes were performed on solvent-extracted, recrystallized waxes, but crystal structure analyses of the natural, mechanically isolated epicuticular waxes are published rarely (e.g. Kreger, 1948; Meusel et al., 2000a). Crystallites of plant epicuticular waxes are not larger than a few μm, thus single-crystal diffraction patterns only can be obtained by electron diffraction. The known crystal structures of waxes (Larsson, 1994) and pure aliphatic wax compounds show a parallel assembly of the straight molecules, whereby molecules of equal length usually form layers (Fig. 1a and b).

In most waxes the molecules are packed in a characteristic order which results in an orthorhombic symmetry of the methylene subcells. However, other symmetries are known; certain wax compounds crystallize preferentially in a triclinic order, and a hexagonal structure occurs often as a high temperature form just below the melting point (further details are given in Section 4). Furthermore, the development of the layer order varies depending on the chain length distribution and the separation of the different components during crystallization. Several types of plant epicuticular waxes show morphological features which seem to be incompatible with a three-dimensional periodical arrangement of the molecules, particularly the wax tubules with a circular cross section and helically grown 'coiled rodlets'.

The intention of the present work was to decide various aspects of the crystal structure: are the plant waxes orthorhombic in general? Are they generally crystalline, particularly the so-called 'amorphous wax films'? Can we recognize specific types of disorder for various wax types? Have the natural waxes the same crystal structure as solvent-extracted, recrystallized wax? Therefore, a new preparation method had been developed which allowed us to examine the native, mechanically isolated waxes and to compare the results with those of solvent-extracted, recrystallized waxes. The knowledge of the crystal structure and disorder will help to understand the crystal growth processes and the properties such as the transpiration barrier function of wax layers and the hydrophobicity and stability of the epicuticular waxes on plant surfaces.

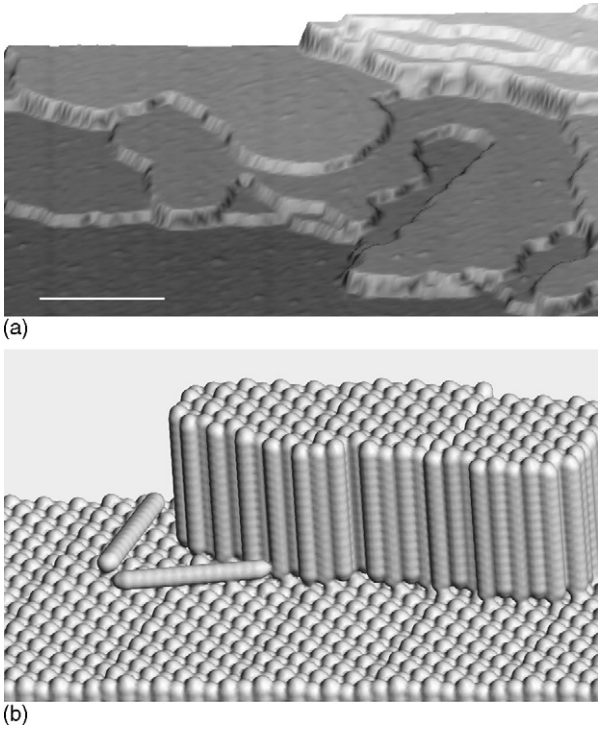

Fig. 1. Typical layer structure of waxes. (a) AFM image of paraffin. (The aspect ratio of the AFM image is not realistic; lateral scan size is 5 μm; height of small steps is ca. 40 Å.) (b) Structure model of an alkane wax. The length of the molecules determines the layer thickness.

2. Materials and methods

2.1. Plant species examined

Epicuticular waxes of the leaves of 32 plant species and three fruits (Table 1) were examined. The plants were cultivated in the Botanical Gardens, University of Bonn (BG Bonn). Apple and vine plants were purchased from 'Pflanzenhof Radermacher', St. Augustin, Germany.

Table 1
Examined species, wax type, melting points of recrystallized waxes, and major components

Species	Wax type	Melting point	Major components, References
Aquilegia canadensis L.	Nonacosanol tubules	76–79 °C	sec. alcohol C29 (1)
Aristolochia tomentosa Sims	Transversaly ridged rodlets	75–76 °C	ketones[b] (2)
Benincasa hispida Thunb.[a]	Longitudinal ridged rodlets	170–180 °C	triterpenol-acetates (3)
Brassica oleracea L.	Dendritic rodlets	65–67 °C	ketones C29, alkanes C29 (4)
Chelidonium majus L.	Nonacosanol tubules	72–73 °C	sec. alcohol C29 (1)
Chrysanthemum segetum L.	Coiled rodlets	64–73 °C	beta-diketone C31 (5)
Convallaria majalis L.	Platelets		prim. alcohol C26, C28, aldehydes, (17)
Crassula ovata Mill.	Crust	77–79 °C	aldehydes C30, C32, alkane C31 (16)
Eucalyptus globulus Labill.	Di-ketone tubules		beta-diketones C33 (6)
Eucalyptus preissiana Schauer	Platelets		prim. alcohols[b] (7)
Euphorbia lathyris L.	Platelets		prim. alcohols C26 (17)
Euphorbia myrsinites L.	Platelets	75–76 °C	prim. alcohol C26, aldehydes (16)
Galanthus nivalis L.	Platelets	71–74 °C	prim. alcohol C26 (17)
Ginkgo biloba L.	Nonacosanol tubules	67–80 °C	sec. alcohol C29 (1)
Gypsophila acutifolia Stev.	Transversaly ridged rodlets	67–68 °C	alkanes C31 (2)
Hedera helix L.	Films		prim. alcohols, aldehydes (8)
Iris germanica L.	Platelets		prim.alcohols C26 (16)
Juniperus communis L.	Nonacosanol tubules	67–70 °C	sec. alkohol C29, hydroxy-fatty acids (9)
Lactuca sativa L.	Films	68–73 °C	prim. alcohols C22, C24, C26 (10)
Lathyrus odoratus L.	Platelets		alkane C31, prim. alcohols C26, C28 (17)
Leymus arenarius L.	Di-ketone tubules	60–67 °C	beta-diketone C31, hydroxy-beta-diketone C31 (5)
Liriodendron chinense (Hemsl.) Sarg.	Transversaly ridged rodlets	76–78 °C	ketones[b] (11)
Magnolia grandiflora L.	Films		fatty acids C24–C30, prim. alcohols C24–C28 (11)
Malus domestica Borkh. cv. Ontario[a]	Platelets, tubules, films	60–63 °C	sec. alcohols, alkanes, acids, esters (12)
Nelumbo nucifera Gaertn.	Nonacosanol tubules	90–95 °C	sec. alkane-diols C29 (13)
Prunus laurocerasus L.	Films		alkanes C29, C31 (14)
Sisyrinchium striatum Sm.	Platelets	78–79 °C	prim. alcohols[b] (16)
Thalictrum flavum glaucum L.	Nonacosanol tubules	73–75 °C	sec. alcohol C29 (13)
Triticum aestivum L. *cv.* Ludwig	Di-ketone tubules		beta-diketone C31 (19)
Triticum aestivum L. cv. Naturastar	Platelets		prim. alcohol C28 (18)
Tropaeolum majus L.	Nonacosanol tubules	74–77 °C	sec. alcohol C29 (4)
Tulipa gesneriana L.	Nonacosanol tubules		sec. alcohol C29 (1)
Vitis vinifera L.[a]	Membraneous platelets	>250 °C	triterpenoides, prim. alcohols (15)
Yucca aloifolia L.	Platelets		prim. alcohols[b] (16)
Yucca filamentosa L.	Platelets		prim. alcohols C28–C32 (16)

Chemical data were obtained from following references: 1: Holloway et al. (1976); 2: Meusel et al. (1999); 3: Meusel et al. (1994); 4: Koch et al. (2006); 5: Meusel et al. (2000b); 6: Horn et al. (1964); 7: Baker (1982); 8: Hauke and Schreiber (1998); 9: Martin and Juniper (1970); 10: Bakker et al. (1998); 11: Gülz et al. (1992); 12: Kolattukudy (1976); 13: Barthlott et al. (1996); 14: Jetter et al. (2000); 15: Casado and Heredia (1999); 16: Haas, K. personal communication; 17: Dommisse, A. personal communication; 18: Koch et al. (2005); 19: Koch, K. unpublished data.

[a] Fruits.

[b] Data from related species with similar waxes.

2.2. Preparation of epicuticular waxes

Mechanical isolation of the intact wax particles or layers was carried out with a cryo-adhesive method, which is described in detail by Ensikat et al. (2000). A piece of a leaf is placed on a preparation liquid, usually triethylene glycol, and then cooled with liquid nitrogen, until the liquid is frozen. After removal of the leaf, the epicuticular wax remains embedded at the surface of the frozen liquid. From some wax types, e.g. platelets and tubules, it is possible to isolate mainly discrete wax particles by using glycerol as preparation liquid. After thawing, the wax can be transferred to other applications. For TEM, the wax on the surface of the drop was touched with a carbon-filmed specimen grid.

For TEM it is sufficient to prepare an area of few mm^2 on a small drop of the preparation liquid. X-ray diffraction requires much more amount of wax (at least 0.1 mg), thus the wax of an area of 20–50 cm^2 was acquired for one sample. To collect the wax, the preparation liquid

with the separated wax was filtered through a 200 mesh metal sieve. Finally, the wax was washed with water and transferred onto the X-ray specimen holder. With a variation of the wax isolation method, the underlying basal wax film was separated from the wax particles grown above: first, the entire wax layer was separated from the leaf with a two-component epoxy glue (Uhu Plus schnellfest, Uhu GmbH, Bruehl, Germany). Then the basal wax film was isolated from the wax-epoxy complex by the cryo-adhesive method, whereby the wax particles remained embedded in the epoxy-glue surface.

From some species with, e.g. very thin or hairy leaves, it is difficult or impossible to prepare sufficient amounts of wax by the cryo-method (Ensikat et al., 2000). Thus, waxes were also collected by extraction with chloroform. The leaves were immersed in chloroform ($CHCl_3$, Merck Darmstadt, Germany) for 5–30 s depending on the solubility of the wax. After evaporation of the solvent, the raw wax was dissolved in warm ethanol; the solution was then filtered and cooled to room temperature at cooling rates between 10 and 2 °C/min. The recrystallized wax was filtered and washed with cold ethanol.

Reference substances: The following substances were used for comparative XRD measurements: Nonacosane (99%), tetracosane (99%), octacosan-1-ol (99%) (all from Sigma, Taufkirchen, Germany), palmitone (99%), paraffin (m.p. 56–58 °C, Merck, Darmstadt, Germany), beeswax (Apiary Goergens, Rommerskirchen, Germany), purified nonacosan-10-ol (98%), isolated from *Tropaeolum majus* leaves (provided by A. Dommisse, Nees Institute for Biodiversity of Plants, Bonn, Germany). The substances were molten on silicon substrates and crystallized at cooling rates of 3–5 °C/s.

2.3. X-ray powder diffraction

Powder diffraction diagrams were recorded with a diffractometer with Bragg-Brentano geometry, PW 1049/10 (Philips, Eindhoven, Netherlands), using Co Kα radiation, wavelength 1.79 Å. The wax quantity varied between 0.2 and 8 mg wax. A silicon plate of $6 \times 10\,mm^2$ was used as substrate. The diffraction diagrams were recorded with steps of $2\theta = 0.02^\circ$ and between 1 and 10 s per step.

2.4. Transmission electron microscopy and electron diffraction

TEM images and diffraction patterns were recorded with two differently equipped microscopes. A CM 300 UT/FEG TEM (Philips, Eindhoven, Netherlands) with a 2 k × 2 k CCD camera (Gatan, München, Germany) was operated at 300 kV. Continuous video records were taken with a CM 120 TEM (Philips, Eindhoven, Netherlands) equipped with a CCD video-camera with image intensifier (Gatan 622 SC). Specimens were examined at room temperature or with a cooling stage at −120 °C. Selected-area diffraction patterns of regions with 2–3 μm in diameter were acquired from single wax particles.

2.5. Determination of melting points

The melting points of the waxes were measured at air on an aluminium plate using a Ni-Cr/Ni thermocouple. The results were checked with reference substances with known melting points.

2.6. Scanning electron microscopy

SEM images were acquired with a Cambridge Stereoscan S 200 (Cambridge, UK). Specimens were sputter-coated with gold.

2.7. Light microscopy

A Zeiss Photomikroskop III (Carl Zeiss GmbH, Oberkochen, Germany) was used for in situ observations of the wax crystallization in solutions.

3. Results

3.1. Reference substances

From several known aliphatic substances XRD diagrams were recorded in order to illustrate the structural characteristics of the waxes (Fig. 2).

The ‘long spacing’-peaks (0 0 *l*) contain information about the thickness and order of the molecular layers. The ‘short spacing’ peaks (*h k* 0), appearing at large diffraction angles, display the lateral packing order of the hydrocarbon chains.

Multi-component waxes (paraffin, beeswax) with molecules of different length exhibit a lower layer order than the pure compounds. This is indicated by a decreased intensity particularly of the higher order (0 0 *l*)-peaks. Pure substances show a long series of (0 0 *l*) peaks, with high intensity for hydrocarbons (nonacosane, tetracosane) and lower intensity, e.g. for primary alcohols. Narrow (0 0 *l*) peaks for octacosan-1-ol indicate a double-layer structure; the decrease of every second (0 0 *l*) peak for palmitone is typical for symmetrical ketones. (Further details of the ‘long spacing’ peaks are explained in Section 4.)

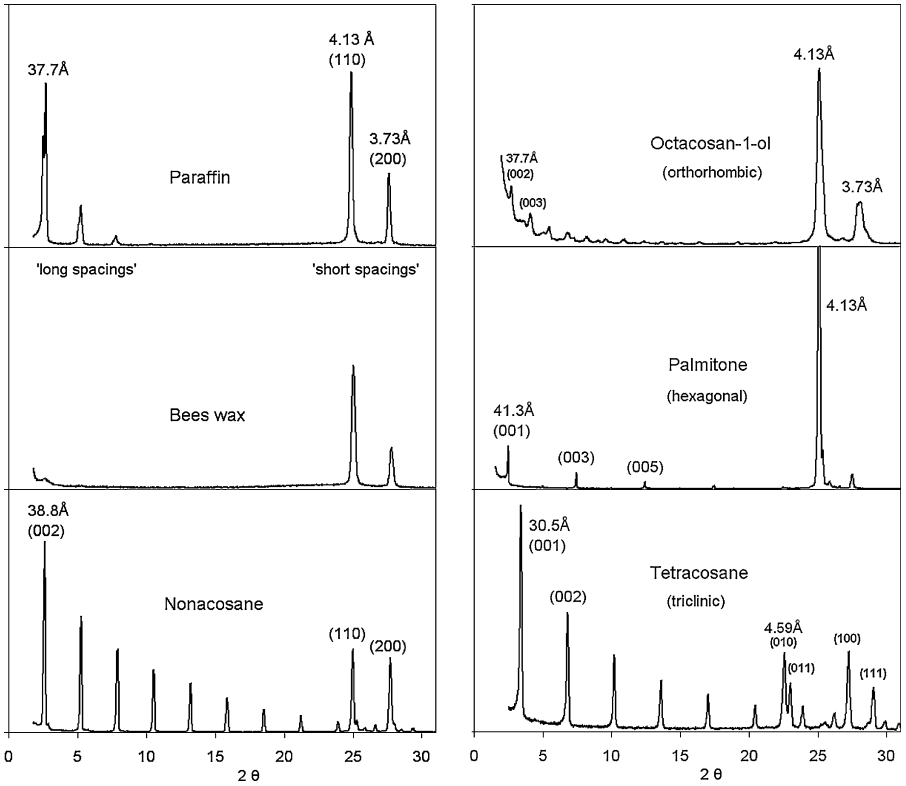

Fig. 2. XRD-diagrams of aliphatic reference substances display various characteristics: Multi-component waxes (paraffin, bees wax) with a low layer order, pure alkanes (nonacosane, tetracosane) with strong (0 0 *l*) peaks, primary alcohols (octacosan-1-ol) with a double layer structure, a ketone (palmitone) with a hexagonal and tetracosane with a triclinic symmetry.

In the 'short spacing' region ($2\theta > 20°$), two intensive peaks corresponding to d-values of 4.13 and 3.72 Å are characteristic for the orthorhombic structure (paraffin, beeswax, nonacosane, octacosan-1-ol). The triclinic structure was found in tetracosane with major peaks of 4.58 and 3.80 Å, whereas the ketone (palmitone) showed only one intensive peak of 4.13 Å, indicating presumably a hexagonal symmetry.

3.2. Plant epicuticular waxes

3.2.1. Platelets

Platelets appear as single particles, clusters or fused aggregates in combination with a basal wax layer. Main components are in most cases primary alcohols.

All examined platelet-waxes showed the two characteristic reflections of the orthorhombic structure corresponding to d-values of 4.13 Å (1 1 0) and 3.73 Å (2 0 0). The recrystallized waxes of *Euphorbia myrsinites* and *Sisyrinchium striatum* (an Iridaceae) showed clear peaks in the 'long spacing' region with a (0 0 1)-spacing of approximately 75 Å, indicating a double layer structure (Fig. 3a). XRD diagrams from recrystallized wax of *Triticum aestivum* var. Naturastar and from *Galanthus nivalis* were almost similar to those of *Sisyrinchium*. Surprisingly, the mechanically isolated waxes of *E. mysinites* and *S. striatum* showed almost no 'long spacing' reflections (Fig. 3), which indicated a significantly lower order of the layer structure.

Electron diffraction from separated single platelets was acquired from *Convallaria majalis*, *Eucalyptus preissiana*, *Euphorbia lathyris*, *Iris germanica*, *Lathyrus odoratus*, *Yucca filamentosa* and *Yucca aloifolia*. Individual platelets usually appear as single crystals (Fig. 4), but sometimes deformations of the platelets cause disturbed diffraction patterns.

3.2.2. Films, layers and crusts

All wax films and crusts examined showed the two characteristic reflections of the orthorhombic structure. In the 'long spacing' region of XRD-diagrams (Fig. 5), very different patterns were found. *Prunus laurocerasus* wax showed clear peaks of medium intensity, similar for mechanically isolated and for solvent-extracted wax.

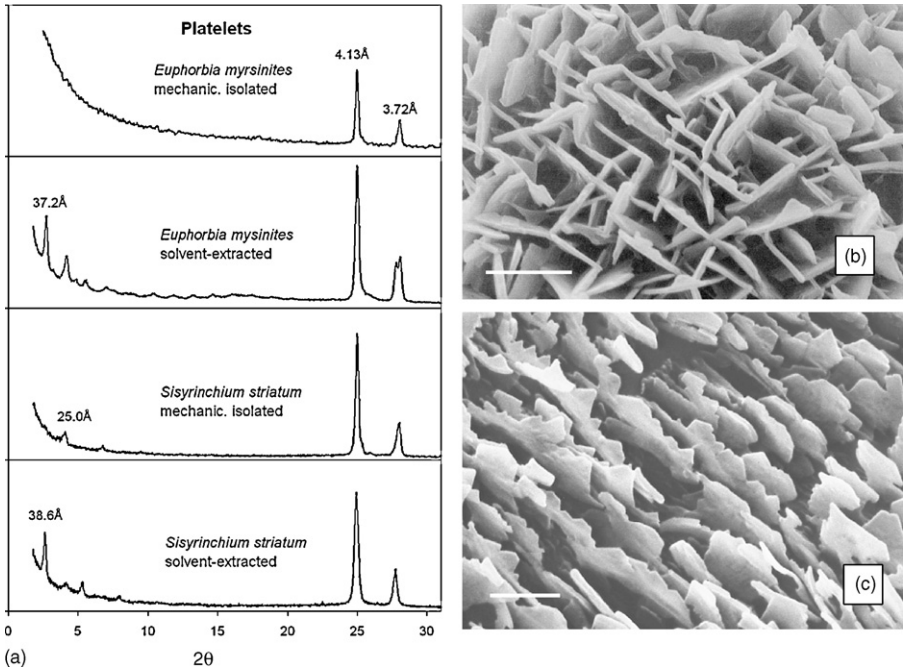

Fig. 3. XRD-diagrams (a) of mechanically isolated and solvent-extracted 'platelet waxes'. The mechanically isolated waxes show almost no 'long spacing' peaks. The peaks of 4.13 and 3.72 Å indicate the orthorhombic symmetry. SEM-images of wax platelets on *E. myrsinites* (b) and *S. striatum* (c) leaves. Bar = 1 μm.

The 'long spacing'-peaks of *Lactuca sativa* (lettuce) were very small, while the mechanically isolated wax crust of *Crassula ovata* showed very intensive peaks with narrow distance indicating a double-layer structure.

Electron diffraction was obtained from mechanically isolated wax films of *P. laurocerasus* (Fig. 6a), *Hedera helix*, *Magnolia grandiflora* and *Vitis vinifera*. All waxes showed the reflections of 4.13 and 3.73 Å indicating an orthorhombic symmetry. Isolated basal wax films from nonacosanol-waxes from *Tulipa gesneriana* and *Thalictrum flavum*, which were separated from the tubules, also showed the diffraction rings corresponding to 4.13 and 3.73 Å (Fig. 6b), but not the 'nonacosanol'-typical reflections of 4.54 Å (see below).

3.2.3. Tubules

Two types of wax tubules different in chemical composition commonly occur: tubules with a high content of secondary alcohols, mainly nonacosan-10-ol and nonacosan-diols ('nonacosanol tubules'), and those with a high content of beta-diketones ('beta-diketone tubules'). In most cases they are associated with a basal wax film, which was found to have an orthorhombic structure (see Section 3.2.2). Both types of tubules

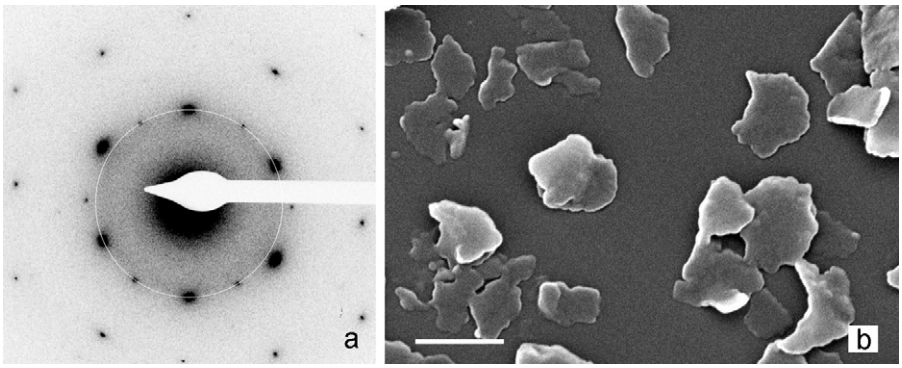

Fig. 4. (a) Electron diffraction of a mechanically isolated single wax platelet of *Yucca filamentosa* showing a single crystal pattern with orthorhombic symmetry. The overlayed white circle marks the d-spacing of 4.13 Å. (b) SEM-image of isolated *Y. filamentosa* platelets. Bar = 1 μm.

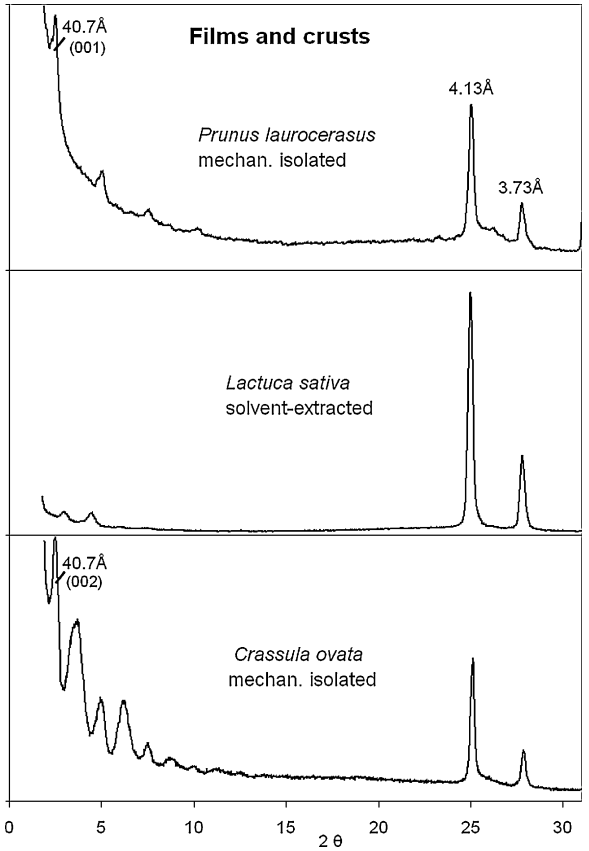

Fig. 5. XRD-diagrams of smooth wax films and crusts. Different intensities of the 'long spacing'-reflections indicate varying development of the layer order; the 4.13 and 3.73 Å reflections represent the orthorhombic symmetry.

showed diffraction patterns which indicate a more or less disturbed crystalline order, but the peaks in the 'short spacing' region indicate structures different from the orthorhombic one (Fig. 7).

The beta-diketone wax of *Leymus arenarius* did not recrystallize in form of tubules; the XRD diagram (Fig. 7) showed a strong 4.13 Å peak, which indicates a hexagonal structure, and a very small 3.8 Å-peak, which may arise from traces of orthorhombic wax. The extinction of the 'long spacing' peaks (0 0 2) and (0 0 4) is characteristic for symmetrical ketones (see Section 4). Electron diffraction patterns of mechanically isolated beta-diketone tubules from *Leymus arenarius*, *T. aestivum*, *Eucalyptus globulus* displayed only the 4.13 Å reflections.

All of the examined 'nonacosanol waxes' occurred as tubules on the plant surface, but they recrystallized in different forms. Waxes of gymnosperms, which consist of nonacosan-10-ol, hydroxy-fatty acids and estolides, recrystallized to sponge-like curled membranes (e.g. *Juniperus communis*, Fig. 8d). The XRD diagram (*J. communis*) shows intensive peaks of the orthorhombic structure and a small peak at 4.54 Å, but the 'long spacing' peaks were virtually absent. The 'nonacosanol waxes' of angiosperm plants (e.g. *Chelidonium*, *Thalictrum*, *Tropaeolum*) recrystallized in ethanol as a mixture of tubules and platelets. XRD diagrams of recrystallized and mechanically isolated wax were almost identical. The 'long spacing'-peaks of tubular 'nonacosanol waxes' (e.g. *Chelidonium majus*) showed the characteristic pattern of nonacosan-10-ol with the extinction of the (0 0 3)- and (0 0 6)-reflections (Fig. 7). The d-spacings were equal to the length of the nonacosan-10-ol

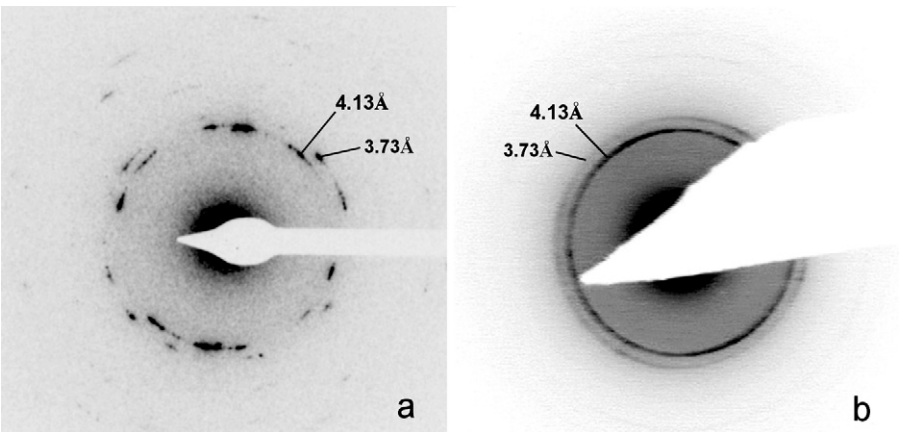

Fig. 6. (a) Electron diffraction pattern of the mechanically isolated wax film of *Prunus laurocerasus*. The discrete reflections indicate relatively coarse crystallites (selected area of approximately 4 μm diameter). (b) The isolated basal wax layer from *Thalictrum flavum* which was separated from the associated tubules, showed the diffraction rings corresponding to 4.13 and 3.73 Å, but not the 'nonacosanol'-typical reflections of 4.54 Å.

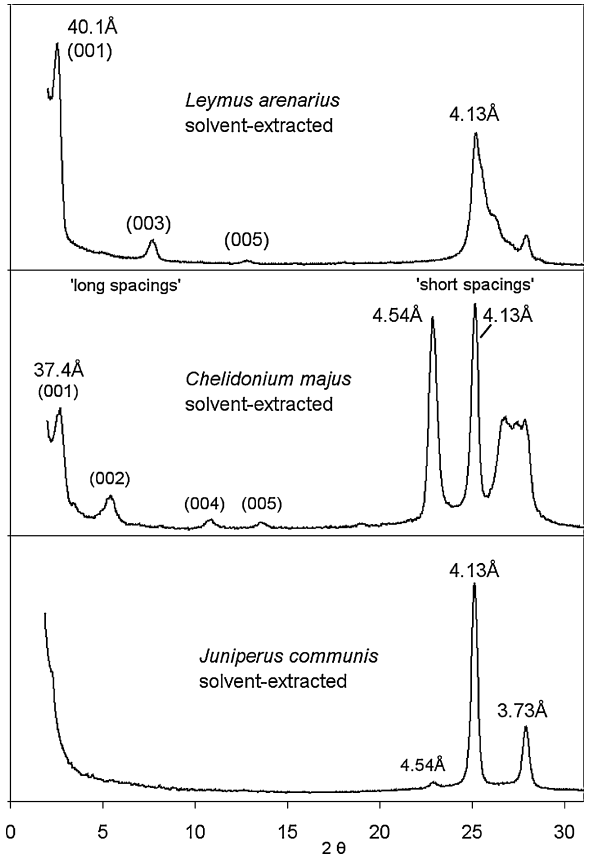

Fig. 7. XRD-diagrams of several tubule-forming waxes: *Leymus arenarius* (beta-diketone wax) shows a strong 4.13 Å peak indicating a hexagonal symmetry; the 'long spacing' peaks are characteristic for symmetrical ketones. *Chelidonium majus* ('nonacosanol-tubules') displays a typical 4.54 Å reflection in addition to the 'orthorhombic' peaks. The extinction of the 'long spacing' peaks (0 0 3) and (0 0 6) identifies nonacosan-10-ol as major component. *Juniperus communis* (recrystallized as curled membranes, Fig. 8d) shows strong peaks of the orthorhombic structure (4.13 and 3.73 Å) and a small 4.54 Å peak, but no 'long spacing'-peaks.

molecules, indicating that they are straight and vertically orientated within the molecular layer.

In the 'short spacing' region (Fig. 9) the 'nonacosanol-tubules' show a characteristic reflection at approximately 4.54 Å and a broad peak, or two peaks close together, between 3.80 and 3.95 Å. These peaks appear additional to the reflections of the orthorhombic structure of 4.13 and 3.73 Å. Different plant species showed a different peak height ratio between the characteristic 'nonacosanol-wax' peaks and the 'orthorhombic' peaks. Pure nonacosan-10-ol, which has been isolated from *T. majus* wax, showed no 'orthorhombic-peaks'; the observed reflections were equivalent to those of tetracosane (Fig. 2) with a triclinic structure. (Differences arise from the larger c-spacing.) The waxes of *Aquilegia canadensis*, *T. flavum* and *C. majus* were obviously mixtures of a triclinic and an orthorhombic phase. This is in agreement with the morphological appearance; the solvent-extracted waxes crystallized in ethanol to a mixture of tubules and platelets or membranes (Fig. 8), and the natural 'nonacosanol'-waxes consisted of tubules and a basal wax film.

The wax of the *Nelumbo nucifera* (Lotus) leaf upside displayed no reflections of the orthorhombic structure. The 4.49 Å-peak is characteristic for the triclinic symmetry, but the broad peak at approx. 3.83 Å indicates a strong disorder. The chemical analysis had shown that this wax consists mainly of nonacosan-diols (personal communication with A. Dommisse).

Electron diffraction patterns of single 'nonacosanol tubules' display details about the disorder. The characteristic 4.54 Å-reflections appeared as streaks or rows of points in a certain orientation (Fig. 10a and b). The corresponding TEM image is inserted in the correct orientation. The streaks appear in almost every orientation of the tubule, due to its circular shape.

3.2.4. Waxes with complex morphologies

Particularly ketone-containing waxes occur in different morphological forms such as transversaly ridged rodlets, coiled, branched and triangular rodlets, usually associated with a basal wax film (Fig. 11).

The XRD diagrams of all examined ketone waxes show the two strong peaks of 4.13 and 3.73 Å of the orthorhombic structure, but the height ratio of the two peaks varied and was in some cases significantly higher than in most other multi-component waxes. In *Liriodendron chinense*-wax for example (Fig. 12), the 4.13 Å-peak was approximately 4.6 times higher than the 3.73 Å-peak; for *Aristolochia tomentosa* the ratio was 4.0, for *Brassica oleracea* approximately 3.8. In contrast, the peak height ratio of other orthorhombic waxes such as paraffin is ca. 3. (Exceptions were found for pure substances.) A sample of pure palmitone, the most common ketone in many waxes, showed in the XRD diagram only one intensive peak at 4.13 Å (see Section 3.1). This leads to the assumption that the very high 4.13 Å-peaks result from a mixture of a hexagonal ketone phase with an orthorhombic phase of other wax components. The 'long spacing'-peaks of *Liriodendron* and *Brassica* showed the characteristic pattern of symmetrical ketones with the decrease of the (0 0 2) and (0 0 4) peaks. The extinction of the (0 0 3)-peak for the *Chrysanthemum* wax matches well with the main component, an asymmetrical ketone (Fig. 12).

Transversaly ridged rodlets are also formed from alkane-rich waxes. The XRD-diagram of *Gypsophila*

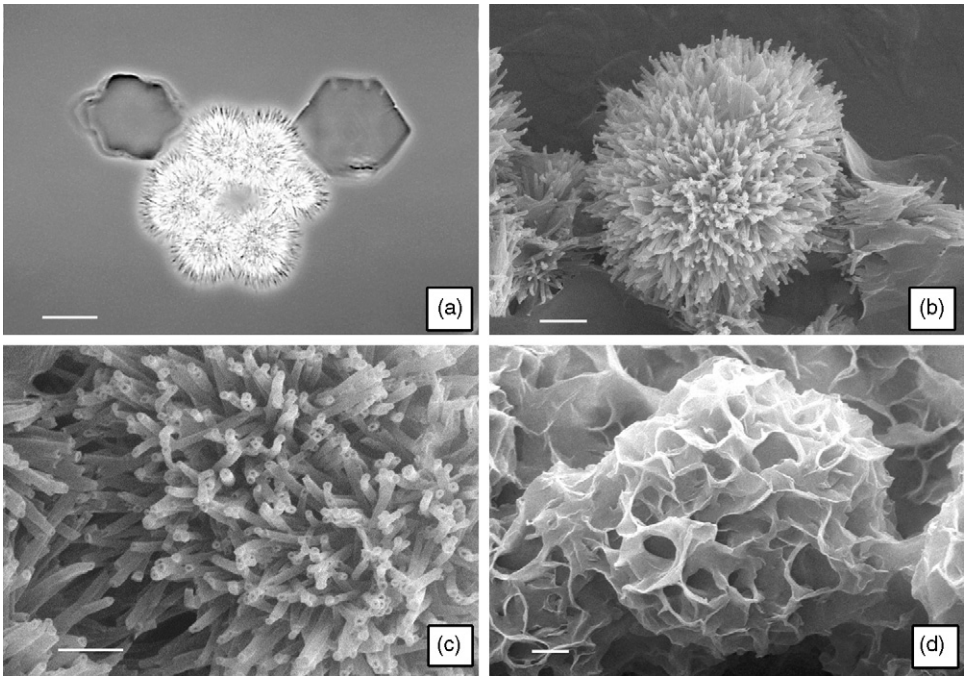

Fig. 8. Recrystallized 'nonacosanol waxes': (a) light microscopic image of *Aquilegia canadensis* wax crystals (tubules and platelets) growing in ethanol; (b, c) SEM images of the spherulite-like aggregates of tubules; (d) SEM image of *Juniperus communis* wax crystallized in ethanol, forming curled membranes (bars: a: 10 μm; b: 2 μm; c: 1 μm; d: 2 μm).

acutifolia wax (Fig. 12) showed an impressive series of 'long spacing' peaks typical for crystals of a pure alkane compound.

3.2.5. Fruit waxes

Apple waxes are mixtures of many components and form diverse wax coatings, e.g. smooth films, oily liquid films (on very ripe fruits) or three-dimensional crystals. Ontario apples (*Malus domestica* cv. Ontario) bear a white wax coating consisting of a mixture of platelets, very short tubules and layers. The XRD diagram (Fig. 13) showed the peaks of the orthorhombic structure and the 4.54 Å peak of 'nonacosanol waxes'. The 'long spacing' peaks indicate a period of 38.3 Å.

The epicuticular coating of grapes (*Vitis vinifera*) forms membraneous platelets and contains a mixture of triterpenoides and aliphatic wax compounds. The properties were different from aliphatic waxes: less soluble in chloroform, a melting point above 250 °C. The chloroform-recrystallized sample showed very broad peaks of non-aliphatic compounds and the two 'orthorhombic'-peaks. In contrast, the mechanically isolated material showed only a small peak at ca. 4.2 Å, indicating that the triterpenoid components were in an amorphous state and the aliphatic components were strongly disordered (Fig. 13).

The thick wax coating of the 'fuzzy melon' *Benincasa hispida* (longitudinal ridged rodlets) also contains triterpenoides, particularly triterpenol-acetates. The XRD diagram of the mechanically isolated material displayed sharp peaks of the same d-spacings as the broad peaks of the grapes wax. The properties resembled more those of normal waxes: better solubility in chloroform and a high melting point of 170–180 °C.

4. Discussion

The present study was performed to obtain an overview over the crystal structures of the different types of epicuticular waxes. The waxes exhibit diverse diffraction patterns, but it was found that the results could be explained with the crystal structures already known from waxes and aliphatic compounds. For the interpretation of the results, the known structure features of aliphatic compounds are presented briefly.

4.1. The established wax structure models

The common crystal structure models of waxes and related aliphatic compounds are established from numerous studies. The following descriptions refer primarily to Larsson (1994), Mazliak (1968) and data from

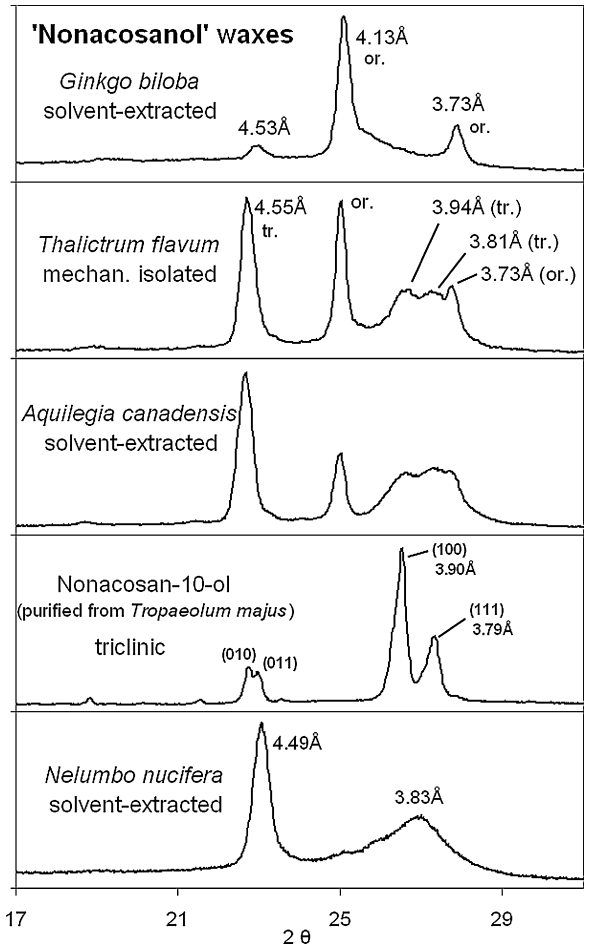

Fig. 9. 'Short spacing' reflections of various 'nonacosanol waxes'. *Thalictrum* and *Aquilegia* wax show reflections of both the assumed triclinic ('tr.') and the orthorhombic ('or.') phase. Pure nonacosan-10-ol and *Nelumbo* wax show the triclinic but no orthorhombic reflections. Recrystallized *Ginkgo* wax contains only small amount of the triclinic phase.

the JCPDS PDF-2 powder diffraction database (ICDD). The model of the parallel assembly of straight aliphatic molecules has been presented in the introduction (Fig. 1a and b). Different crystal structure symmetries of the methylene subcells occur, when molecules take different orientations relative to their neighbours by rotation around their long axis (Larsson, 1994). In the orthorhombic structure the C-C zig-zag planes of the molecules occur in two orientations, almost perpendicular to their neighbours (Fig. 14a and b). Two other basic symmetries are described in the literature. A hexagonal structure occurs often at higher temperatures, just below the melting point. Here the molecules are oriented in three directions or they can rotate around the long axis (rotator phase). A triclinic symmetry (or monoclinic, if the angles α and γ are 90 °C) is found, e.g. in pure *n*-alkane compounds with even number of carbon chain lengths (Dorset, 2001). In this structure the zig-zag planes are oriented parallel (Fig. 14c).

4.2. Explanation of the XRD-diagram features

The 'long spacing' peaks provide information about the layer order. The d-value of the (0 0 1)-reflection represents the thickness of the molecular layers The length of alkane molecules with *n* carbon atoms can be calculated by the formula $(1.273n + 1.875)$ Å (Dorset, 1995). A series of higher order (0 0 *l*)-reflections indicates a regular, periodic structure.

In the case of alkanes, for example, the series of (0 0 *l*)-peaks originates from the region of lower scattering density in the gap between the molecular layers. Note that the sharp diffraction reflections do not represent the thickness of a single layer, but the periodical sequence of density differences in multiple layers.

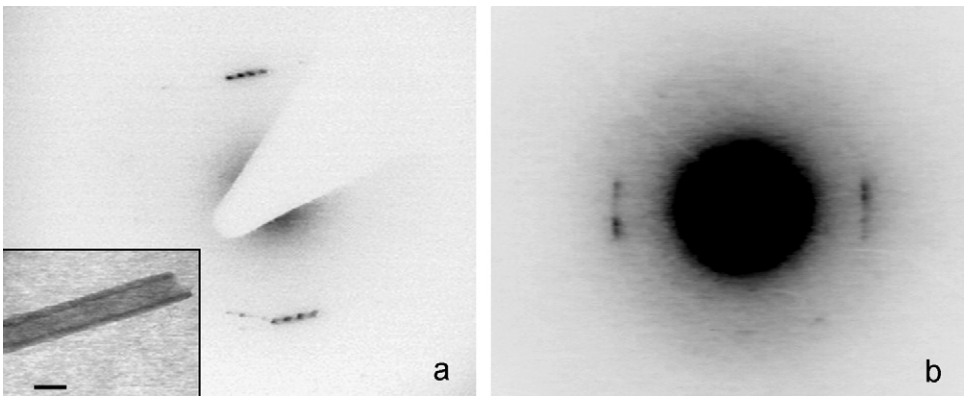

Fig. 10. ED patterns of single nonacosanol tubules (a: *Thalictrum flavum*, b: *Aquilegia canadensis*) show typically streaks or rows of reflexes at a d-spacing of 4.54 Å (inserted image: bar = 100 nm).

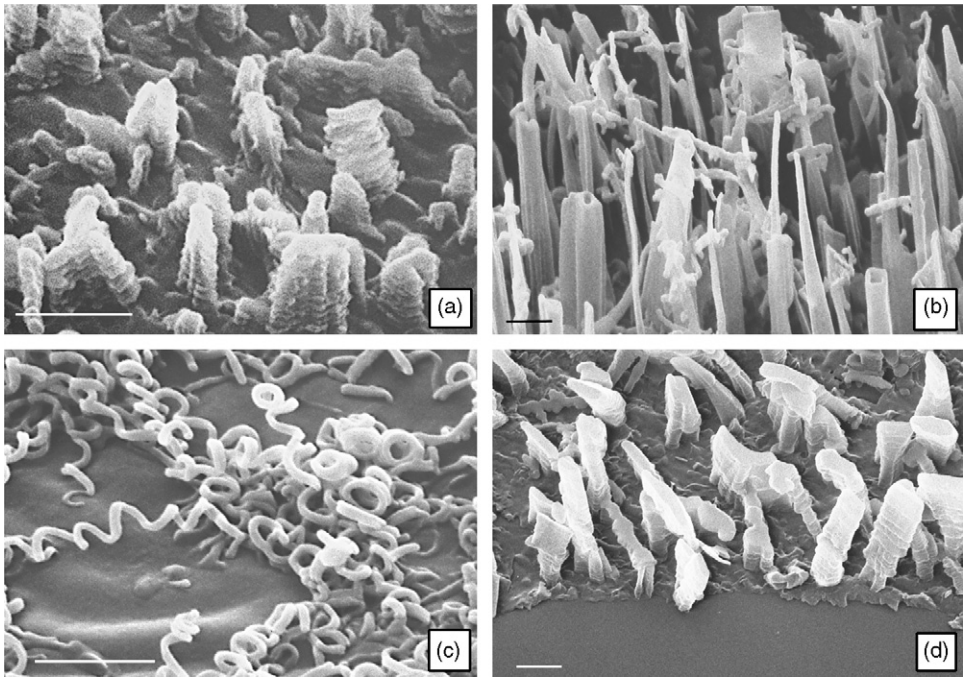

Fig. 11. SEM images of epicuticular waxes with complex morphologies. (a) *Liriodendron chinense* (transversaly ridged rodlets), (b) *Brassica oleracea* (angular tubules with branches), and (c) *Chrysanthemum segetum* (coiled rodlets) contain ketones; (d) *Gypsophila acutifolia* wax (transversaly ridged rodlets) consists of alkanes. At the edge of the removed wax layer, the basal wax film can be clearly recognized. Bar = 1 μm.

Reduced intensities of the 'long spacing' peaks may have several reasons:

1. no layer order (nematic phase): no (0 0 *l*)-peaks detectable;
2. layers of different thickness are stacked: the (0 0 1)-peak may be intensive; the intensity of higher-order peaks decreases rapidly;
3. the density difference of the gap region is low, when the lower density of the gap is compensated by additional oxygen atoms, e.g. in primary alcohols: all (0 0 *l*)-peaks have low intensity, but the higher order peaks are detectable.

Double layer structures result, when compounds with polar groups at the end of the molecules assemble with a head-to-head orientation; the diffraction peaks appear at the half 2θ angle.

The reduced intensity or even extinction of certain (0 0 *l*)-reflections is characteristic for some compounds which occur commonly in plant waxes, particularly for symmetrical ketones and beta-diketones and for nonacosan-10-ol. It is caused by oxygen atoms at a specific position in the long-chain molecules. In the crystal, these oxygen atoms form a plane of higher scattering density which lies between the planes of lower density. The planes of higher and lower scattering density cause a destructive interference of the X-rays (or electrons) for certain peaks, which can be calculated by simulation software or Fourier transformation. It may become comprehensible with the following explanation:

In an alkane crystal, the (0 0 *l*)-reflections originate from the region of lower density between the molecular layers. If, theoretically, in the middle of each layer atoms would be removed and the local scattering density decreases, the structure would be converted to a layer structure with half the thickness. Thus, every second diffraction peak ((0 0 2), (0 0 4) . . .) would increase, the other ones would decrease. In the case of the wax compounds, for example symmetrical ketones, the contrary effect occurs. Additional oxygen atoms cause a higher density in the middle of each layer; consequently every second diffraction peak decreases. In the case of nonacosan-10-ol, the additional oxygen-atoms are at a position of one-third of the molecule length. This causes, analogical, a decrease of every third peak ((0 0 3), (0 0 6)).

4.3. Observed variability of wax morphology and crystal structure

In the typical growth of wax crystals, straight aliphatic molecules assemble preferentially side by side and form layers or platelets, since the growth speed is highest in

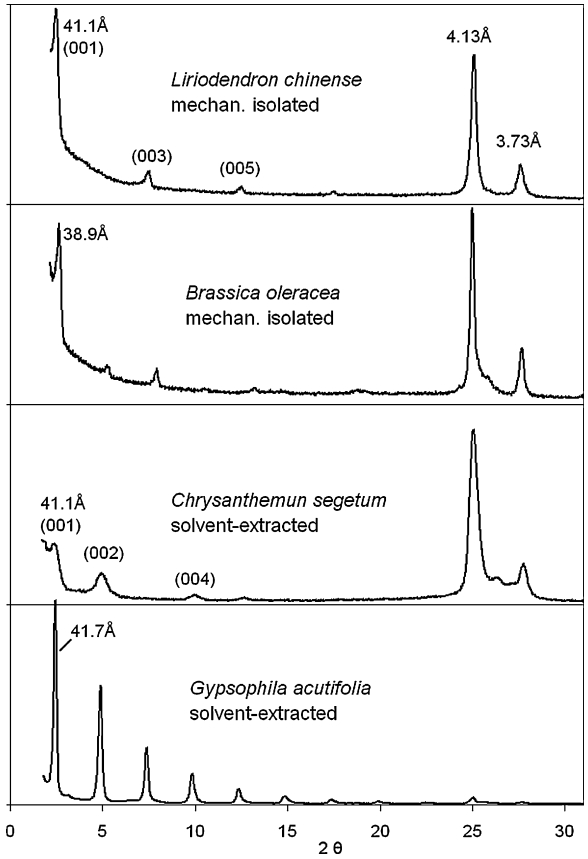

Fig. 12. XRD-diagrams of ketone- and alkane-waxes. The intensity ratio of the 4.13 and 3.73 Å-reflections is particularly for *Liriodendron* and *Chrysanthemum* wax higher than for most orthorhombic waxes. The 'long spacing' peaks indicate a distinct layer order and show the characteristics of the major components. *Gypsophila acutifolia* wax shows the pattern of an almost pure alkane. The low intensity of the 'short spacing' peaks may be a result of a preferential orientation of the crystals.

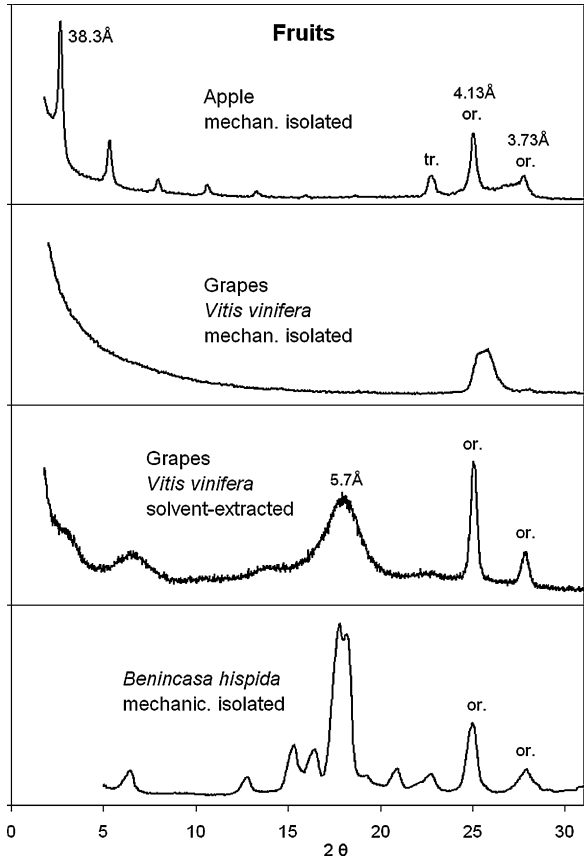

Fig. 13. XRD-diagrams of fruit waxes. Wax of Ontario-apples consists of platelets, 'nonacosanol-tubules' and layers. The solvent-extracted, recrystallized wax of grapes shows sharp reflections of the orthorhombic structure and broad diffuse peaks of the triterpenoid components. The mechanically isolated grapes wax display only one diffuse peak like a hexagonal aliphatic phase; the triterpenoid components are obviously amorphous. The wax of *Benincasa hispida* shows the reflections of orthorhombic wax and sharp reflections of the triterpenoid components.

the lateral direction (Dorset et al., 1983). Pure compounds usually form regular crystals with a periodic order in three dimensions. However, the plant waxes are mixtures of several compounds. If single components dominate, they may form separate crystals, while minor constituents remain mixed as a solid solution. Waxes with a low layer order often seem to be mixtures of compounds with varying chain length.

Great variations in the crystal morphology were found in waxes which contain components with lateral oxygen atoms as ketones and secondary alcohols. These components apparently hinder the formation of the orthorhombic structure, as the oxygen atoms require additional space. In the case of the tubular waxes, even the formation of a periodic crystal lattice is inhibited; the tubules grow with a circular or helical shape. Broad diffraction peaks indicate a short-range order, but on a larger scale, the tubules consist of an aperiodic arrangement of molecules. 'Nonacosanol-tubules' show the characteristic diffraction peaks of triclinc alkanes, beta-diketone tubules only one intensive peak like hexagonal waxes. However, due to the aperiodic tubular structure it may be incorrect to declare these structures as regular triclinic or hexagonal. Nevertheless, we used these terms to assign the peaks in the diffraction diagrams. Models for the crystal structure of nonacosan-10-ol, based on regular periodic structures, have been proposed by Jetter and Riederer (1994) and Matas et al. (2003). However, these models did not sufficiently explain the formation of the curvature of the tubule walls. However, the triclinic structure on its own is not the reason for the formation of the tubules; the triclinic structure also occurs in regular alkane crystals. Further studies may clarify whether the

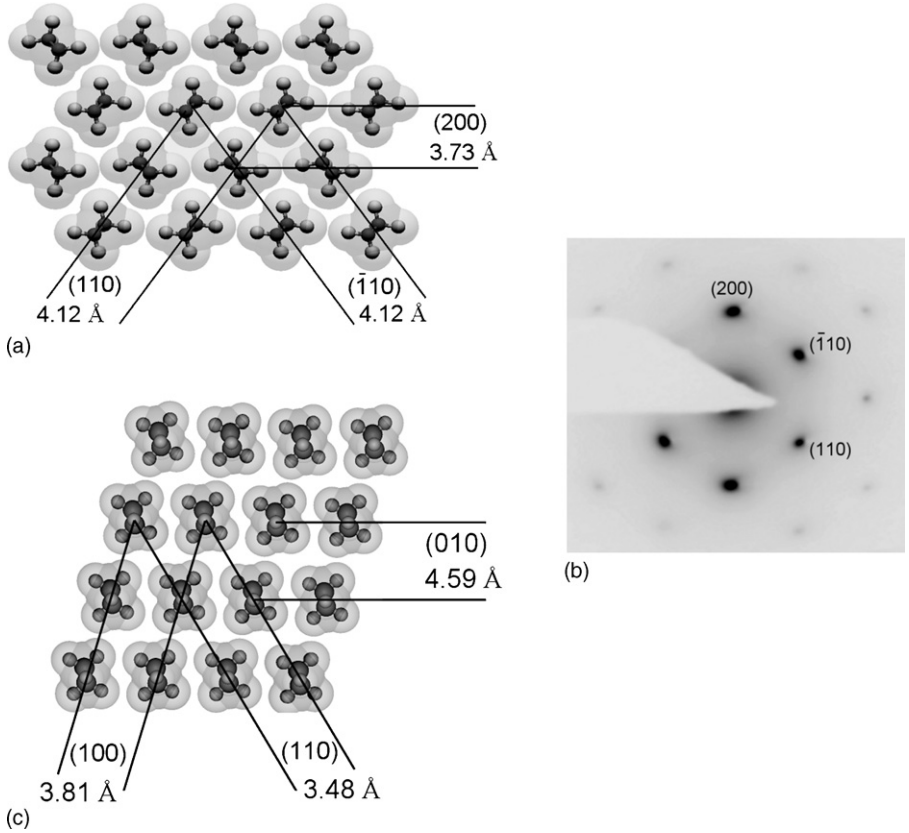

Fig. 14. Models of the orthorhombic and triclinic symmetry of the methylene subcells. (a) The orthorhombic structure: view along the long axis of the hydrocarbon molecules; (b) single crystal electron diffraction pattern of octacosan-1-ol with Bragg reflections corresponding to the orthorhombic structure in (a). (c) Model of the triclinic symmetry. Indices and d-spacings are taken from PDF-files of *n*-Nonacosane (40-1997) and *n*-Tetracosane (40-1998) (JCPDS 1999).

chirality of the molecules or other factors are determining for the tubule growth.

For the 'nonacosanol-waxes' it became clear that they mostly consist of a mixture of two phases, the 'triclinic' one and orthorhombic, which could be distinguished by characteristic diffraction peaks. In the case of ketone-rich waxes, it is less clear, since the 'hexagonal'-peak has the same d-value as the (1 1 0)-peak of the orthorhombic phase. Thus, the content of a hexagonal ketone phase was only indicated by the exceeding intensity ratio of the (1 1 0) and (2 0 0)-peaks and by the fact that pure palmitone was found to form a hexagonal phase. (Under different crystallization conditions, we found palmitone and tetracosane also with an orthorhombic structure.)

In several studies the morphology of natural and recrystallized wax of the same species have been compared, with the aim to reproduce the original shape and to understand the crystallization processes in detail (Meusel, 1997; Jetter and Riederer, 1994; Jeffree et al., 1975). It was found that certain waxes can crystallize in different forms, depending on the conditions. Jetter and Riederer (1994) demonstrated that pure S-nonacosan-10-ol could form tubules as well as flat platelets. However, the crystallization conditions on the plant surfaces are unique, as the wax molecules move relatively slowly from inside of the leaf through the cuticle and crystallize without a solvent on the dry surface. In this natural system the speed of the crystal growth is determined by the speed of wax synthesis and transport (Koch et al., 2004). For this study, we did not particularly try to copy the natural morphology; the solvent-extracted waxes were used as they resulted from the purification by recrystallization with ethanol. In many cases, they grew in similar forms as on the plant surface, for example 'nonacosanol'-tubules. In most cases, the recrystallized waxes displayed a similar diffraction diagram as the mechanically isolated ones, but in several cases the latter ones had a remarkably lower order (e.g. platelets). This is not surprising, since on the dry plant surface the crystallization conditions are far from an equilibrium state and the mobility of the molecules is much lower than in a solution. It also may be possible, that the crystal structure has been degraded

by ageing processes, i.e. chemical alterations such as oxidation, polymerization, or influence of UV-radiation.

4.4. Suitability of the methods

The present study primal became possible with the availability of the new 'cryo-adhesion' preparation method, which preserves the crystal structure and isolates the epicuticular waxes selectively. It is known that chloroform-extracts contain to some extent intracuticular or even cytoplasmic contents. The solvent-extracted waxes of this study usually were yellow-coloured, whereas the mechanically isolated waxes appeared colourless. Jetter et al. (2000) demonstrated that mechanically isolated wax from *P. laurocerasus* leaves was free from triterpenoides, which abounded in the chloroform extracts. The 'cryo-adhesion' method also receives insoluble or slowly soluble components, which may be lost with the solvent-extraction. Haas et al. (2001) reported, that particularly aldehyde-rich waxes, e.g. from rice and sugar cane, are almost insoluble in chloroform at ambient temperature, and warm chloroform is necessary to dissolve them. However, for several species the cryo-adhesion method was not successful. Waxes isolated from leaves with a hairy or papillose surface (*N. nucifera*, *Euphorbia myrsinites*) often contained too much debris of the leaves. For small or fragile leaves and for conifer needles the procedure can be extremely time-consuming.

Due to the small size of the wax crystals, diffraction patterns from single wax particles could be obtained only by electron diffraction. Powder diffraction diagrams were preferentially acquired by XRD because it provided quantitative data with much better quality than ED. The detection of small or broad diffraction peaks was less reliable with ED due to a higher background signal from the supporting film and possible damages of the crystal structure by the electron beam.

The presented results give an overview over the most representative structures of the aliphatic epicuticular waxes and have revealed a remarkable variability. However, the value of diffraction methods for the study of aperiodic structures is limited, thus other techniques may be necessary to elucidate the molecular order. High resolution TEM imaging is, however, severely restricted, but with a scanning tunnelling microscope (STM) individual wax molecules can be observed (De Feyter and De Schryver, 2003). Real time AFM investigations of the formation of wax layers and three-dimensional crystals (Koch et al., 2004) seem to be an appropriate method to get more details about the structural development and stability of the waxes.

Acknowledgments

We thank the Deutsche Forschungs Gemeinschaft and the University of Bonn for the financial support of our research and Dr. K. Haas (Institut für Botanik, Hohenheim) for the support of wax chemical composition data; Dipl. Chem. A. Dommisse (Nees-Institut für Biodiversität der Pflanzen, Bonn) for provision of purified wax compounds and chemical analysis of wax composition. We acknowledge the technical assistance of Prof. V. Herzog (Institute of Cell Biology, University of Bonn) and Dr. B. Buchen (Institut für Zelluläre und Molekulare Botanik, Bonn) and are very grateful for the advices of Prof. H. Klapper (Institut für Kristallographie, RWTH Aachen).

References

Baker, E.A., 1982. Chemistry and morphology of plant epicuticular waxes. In: Cutler, D.F., Alvin, K.L., Price, C.E. (Eds.), The Plant Cuticle. Academic Press, London, pp. 139–165.

Bakker, M., Baas, W., Sijm, D., Kollöffel, C., 1998. Extraction and identification of leaf wax of *Lactuca sativa* and *Plantago major*. Phytochemistry 47, 1489–1493.

Barthlott, W., Neinhuis, C., 1997. Purity of the sacred lotus, or escape from contamination in biological surfaces. Planta 202, 1–8.

Barthlott, W., Neinhuis, C., Cutler, D., Ditsch, F., Meusel, I., Theisen, I., Wilhelmi, H., 1998. Classification and terminology of plant epicuticular waxes. Bot. J. Linn. Soc. 126, 237–260.

Barthlott, W., Neinhuis, C., Jetter, R., Bourauel, T., Riederer, M., 1996. Waterlily, poppy, or sycamore: on the systematic position of *Nelumbo*. Flora 191, 169–174.

Casado, C., Heredia, A., 1999. Structure and dynamics of reconstituted cuticular waxes of grape berry cuticle (*Vitis vinifera* L). J. Exp. Botany 331, 175–182.

De Feyter, S., De Schryver, F., 2003. Two-dimensional supramolecular self-assembly probed by scanning tunneling microscopy. Chem. Soc. Rev. 32, 139–150.

Dorset, D., 1995. The crystal structure of waxes. Acta Cryst. B51, 1021–1028.

Dorset, D., 2001. From waxes to polymers—crystallography of polydisperse chain assemblies. Struct. Chem. 13, 329–337.

Dorset, D., Pangborn, W., Hancock, A., 1983. Epitaxial crystallization of alkane chain lipids for electron diffraction analysis. J. Biochem. Biophys. Meth. 8, 29–40.

Ensikat, H., Neinhuis, C., Barthlott, W., 2000. Direct access to plant epicuticular wax crystals by a new mechanical isolation method. Int. J. Plant Sci. 161 (1), 143–148.

Gülz, P., Müller, E., Schmitz, K., 1992. Chemical composition and surface structures of epicuticular leaf waxes of *Ginkgo biloba*. Magnolia grandiflora and Liriodendron tulipifera. Z. Naturforsch. 47c, 516–526.

Haas, K., Brune, T., Rücker, E., 2001. Epicuticular wax crystalloids in rice and sugar cane leaves are reinforced by polymeric aldehydes. J. Appl. Bot. – Angew. Bot. 75, 178–187.

Hauke, V., Schreiber, L., 1998. Ontogenetic and seasonal development of wax composition and cuticular transpiration of ivy (*Hedera helix* L.) sun and shade leaves. Planta 207, 67–75.

Holloway, P., Jeffree, C., Baker, E., 1976. Structural determination of secondary alcohols from plant epicuticular waxes. Phytochemistry 15, 1768–1770.

Horn, H., Kranz, Z., Lamberton, J., 1964. The composition of *Eucalyptus* and some other leaf waxes. Aust. J. Chem. 17, 464–476.

Jeffree, C., 1996. Structure and ontogeny of plant cuticles. In: Kerstiens, G. (Ed.), Plant Cuticles. Bios Scientific Publishers, Oxford, pp. 33–81.

Jeffree, C., Baker, E., Holloway, P., 1975. Ultrastructure and recrystallization of plant epicuticular waxes. New Phytol. 75, 539–549.

Jetter, R., Riederer, M., 1994. Epicuticular crystals of nonacosan-10-ol: in-vitro reconstitution and factors influencing crystal habits. Planta 195, 257–270.

Jetter, R., Schäffer, S., Riederer, M., 2000. Leaf cuticular waxes are arranged in chemically and mechanically distinct layers: evidence from *Prunus laurocerasus* L. Plant Cell Environ. 23, 619–628.

Koch, K., Barthlott, W., Koch, S., Hommes, A., Wandelt, K., Mamdouh, W., De-Feyter, S., Broekmann, P., 2006. Structural analysis of wheat wax (Triticum aestivum): from the molecular level to three dimensional crystals. Planta 223, 258–270.

Koch, K., Hartmann, K., Schreiber, L., Barthlott, W., Neinhuis, C., 2005. Influence of air humidity on epicuticular wax chemical composition, morphology and wettability of leaf surfaces. J. Environ. Exp. Bot. 56, 1–9.

Koch, K., Neinhuis, C., Ensikat, H., Barthlott, W., 2004. Self assembly of epicuticular waxes on living plant surfaces imaged by atomic force microscopy (AFM). J. Exp. Bot. 55, 711–718.

Kolattukudy, P., 1976. Chemistry and biochemistry of natural waxes. Elsevier, Amsterdam.

Kreger, D., 1948. An X-ray study of waxy coating from plants. Recueil des Traveaux botaniques Neerlandais 42, 606–736.

Larsson, K., 1994. Lipids: Molecular Organization, Physical Functions and Technical Applications. The Oily Press, Dundee.

Malkin, T., 1952. The molecular structure and polymorphism of fatty acids and their derivates. Progr. Chem. Fats 1, 1–17.

Martin, J., Juniper, B., 1970. The Cuticle of Plants. Edward Arnold, London.

Matas, A., Sanz, M., Heredia, A., 2003. Studies on the structure of the plant wax nonacosan-10-ol, the main component of epicuticular wax conifers. Int. J. Biol. Macromol. 33, 31–35.

Mazliak, P., 1968. Chemistry of Plant Cuticles. Progress in Phytochemistry, vol. 1. Interscience Publishers, New York, pp. 49–111.

Meusel, I., 1997. Mikromorphologie, Chemie und in-vitro-Kristallisation epicuticularer Wachse und ihre Anwendung in der Systematik. Ph. D. thesis, University Bonn.

Meusel, I., Barthlott, W., Kutzke, H., Barbier, B., 2000a. Crystallographic studies of plant waxes. Powder Diffr. 15 (2), 123–129.

Meusel, I., Leistner, E., Barthlott, W., 1994. Chemistry and micromorphology of compound epicuticular wax crystalloids (Strelitzia-type). Plant Syst. Evol. 193, 115–123.

Meusel, I., Neinhuis, C., Markstädter, C., Barthlott, W., 1999. Ultrastructure, chemical composition, and recrystallization of epicuticular waxes: transversely ridged rodlets. Can. J. Bot. 77, 706–720.

Meusel, I., Neinhuis, C., Markstädter, C., Barthlott, W., 2000b. Chemical composition and recrystallization of epicuticular waxes: coiled rodlets and tubules. Plant Biol. 2, 462–470.